*Antibodies* **2015**, *4*, 71-87; doi:10.3390/antib4020071

OPEN ACCESS

*antibodies*

**ISSN 2073-4468**

www.mdpi.com/journal/antibodies

*Article*

# A Monoclonal Antibody to Human DLK1 Reveals Differential Expression in Cancer and Absence in Healthy Tissues

**Emil Bujak [1,2], Danilo Ritz [2] and Dario Neri [1,*]**

[1] Department of Chemistry and Applied Biosciences, Swiss Federal Institute of Technology (ETH Zürich), Vladimir-Prelog-Weg 2, CH-8093 Zurich, Switzerland; E-Mail: emil.bujak@pharma.ethz.ch

[2] Philochem AG, Libernstrasse 3, CH-8112 Otelfingen, Switzerland; E-Mail: danilo.ritz@philochem.ch

* Author to whom correspondence should be addressed; E-Mail: neri@pharma.ethz.ch; Tel.: +41-44-3422559; Fax: +41-44-6331358.

Academic Editor: Ahuva Nissim

*Received: 18 November 2014 / Accepted: 8 April 2015 / Published: 16 April 2015*

**Abstract:** There is considerable interest in the characterization of novel tumor-associated antigens that lend themselves to antibody-mediated pharmacodelivery strategies. Delta-like 1 homolog protein (DLK1), which exists both as transmembrane protein and in soluble form, shows a restricted pattern of expression in healthy organs, while being overexpressed in some tumors. We have generated a human antibody specific to DLK1 using phage display technology. This reagent was used for a comprehensive characterization of DLK1 expression in freshly frozen sections of normal human adult tissues and of xenografted human tumors. DLK1 was virtually undetectable in most organs, except for placenta which was weakly positive. By contrast, DLK1 exhibited a moderate-to-strong expression in 8/9 tumor types tested. Our analysis shed light on previous conflicting reports on DLK1 expression in health and disease. The study suggests that DLK1 may be considered as a target for antibody-mediated pharmacodelivery strategies, in view of the protein's limited expression in normal tissues and its abundance in the interstitium of neoplastic lesions.

**Keywords:** DLK1; antibody; phage display; immunostaining; small immune protein (SIP); pharmacodelivery; tumor targeting

## 1. Introduction

Monoclonal antibodies represent the fastest growing segment of pharmaceutical biotechnology products [1,2]. At present, almost 80% of the worldwide antibody sales target only five antigens [3], but there is a growing interest in the characterization of disease-associated antigens that may be used for the development of antibody-mediated pharmacodelivery and pharmacotherapy strategies.

Human DLK1 (protein delta homolog 1) exists as a transmembrane protein, but, upon cleavage by the ADAM17 protease, it may be released as a soluble protein [4]. The structure of DLK1 reveals six epidermal growth factor (EGF)-like extracellular domains, a juxtamembrane region containing the ADAM17 cleavage site, a transmembrane domain and a short intracellular region [5]. DLK1 has been shown to inhibit Notch activity, controlling a wide range of developmental processes including cell fate determination, terminal differentiation and proliferation [6,7]. Both transmembrane and soluble forms of DLK1 are active [8] and are involved in adipogenesis [9], muscle development and injury healing [10], as well as in the development of liver [11], lung and pancreas [12].

In murine tissues, DLK1 is predominantly expressed in many fetal tissues and in non-differentiated cells, while being almost virtually absent from adult tissues with the exception of adrenal gland, as demonstrated by the expression analysis of DLK1 mRNA [9]. In human tissues, DLK1 expression is most pronounced in the embryonic period as well, exhibiting negative correlation with the increased level of cellular differentiation and fetal development [13]. In adult human tissues DLK1 expression is restricted to pancreas [14] and adrenal gland [15], while being almost absent in other tissues [16]. However, DLK1 mRNA expression is also observed in ovary, testis, heart and pituitary gland [17]. DLK1 may also be expressed by some stem cells such as preadipocytes and neuron stem cells [18,19]. DLK1 pattern of expression as well as its role in the Notch pathway implies antigen's involvement in maturation of several tissues. However, DLK1-null mice display mild phenotype with growth retardation, skeletal malformation and increase in serum lipid metabolites [20–22].

As the dysregulation of imprinted genes may contribute to oncogenesis, up-regulation of DLK1, a paternally imprinted gene, may contribute to human hepatocellular carcinoma [23] and DLK1-positive patients have a shorter survival time [24]. The expression of DLK1 has also been reported in small cell lung carcinoma [5], renal cell carcinoma [25], neuroblastoma [26], hepatoblastoma [27], in myelodysplastic syndromes [28,29], pituitary tumors [30], as well as breast, colon and prostate carcinomas [31]. However, other reports indicated a low DLK1 expression in pancreatic, breast and ovarian cell lines [32]. Expression of DLK1 in healthy tissues is predicted to be low, as indicated by mRNA analysis [16].

DLK1 overexpression was shown to promote tumor cell growth in mice [23,33,34]. However, other studies have reported that exogenous expression of DLK1 may inhibit tumor growth *in vitro* [35,36]. DLK1 expression is induced in hypoxic regions of certain brain tumors, possibly contributing to the invasive potential of cancer cells. The cytoplasmic domain of DLK1 appears to be particularly important for maintaining clonogenicity and tumorogenicity [34]. It seems that DLK1 can exert either oncogenic or tumor suppressor effect in tumor depending on its expression level and the effect it has on Notch signaling in a particular tumor type [7,37].

The Protein Atlas Project is the first genome-wide initiative aiming at documenting comprehensive protein tissue expression by means of immunohistochemical analysis [38]. In healthy tissues, various degrees of DLK1-staining were observed in pancreas, uterus, kidney, testis, nasopharynx, bronchus and

cerebellum. Strong nuclear staining was shown in few cancer types and in only a small number of patients. However, the reported staining patterns were different, depending on the antibody that was used for the analysis. Indeed, three different antibodies produced concordant results only for the staining of the adrenal gland, while staining results were ambiguous for other normal tissues and pathological specimens.

DLK1 may be an attractive antigen for antibody-mediated tumor targeting due to its tumor-restricted expression pattern, as well as due to an often perivascular localization which makes DLK1 readily accessible via deregulated tumor vasculature [25]. In fact, vaccination of renal cell carcinoma-bearing mice against DLK1 elicited an immune-mediated elimination of DLK1-positive pericytes, blood vessel normalization and tumor growth suppression [25]. This report motivated us to generate fully human antibodies against DLK1 and to characterize staining patterns in freshly frozen tissue sections. Our laboratory has extensively worked on the use of vascular targeting antibodies for pharmacodelivery applications [39–41].

Phage display technology is a powerful tool allowing for the isolation of fully human high affinity antibodies against virtually any target. We have recently described the generation of a large synthetic naïve phage display library containing 40 billion clones [42]. We used our libraries to generate a high affinity antibody, which recognizes human DLK1 in ELISA, BIAcore and on frozen tissues. An immunofluorescence analysis of human healthy tissues as well as human cancer xenograft specimens revealed that DLK1 is virtually undetectable in normal adult tissues, while being strongly expressed in neoplastic lesions.

## 2. Results and Discussion

### *2.1. Antigen Expression and Characterization*

An extracellular part of the protein, comprising 6 EGF-domains and a juxtamembrane domain, was cloned as a fusion with the Fc portion of human IgG1 and expressed in HEK293-EBNA cells (Figure 1a,b and Supplementary Figure S1). The protein was purified from culture supernatants using Protein A resin, yielding preparations of acceptable quality for subsequent antibody selection experiments, as demonstrated by SDS-PAGE and FPLC analysis (Figure 1c,d).

The mass spectrometry analysis confirmed the identity of the human DLK1 protein in the expressed DLK1-Fc fusion protein (Table 1). The purified DLK1-Fc fusion protein was biotinylated and used for the selection experiments with combinatorial antibody phage display libraries.

### *2.2. Antibody Isolation and Characterization*

A human monoclonal antibody (termed EB3) in single-chain Fv format (scFv) [43], which strongly reacted with recombinant DLK1, was isolated from the ETH2-GOLD antibody library [44] after three rounds of panning (Supplementary Figure S1).

The EB3 antibody was reformatted as a small immune protein (SIP) [45]. A monomeric preparation of scFv(EB3), as well as the same antibody in SIP format, were studied using BIAcore technology on a microsensor chip coated with the DLK1-Fc fusion protein (Figure 2, Supplementary Figure S2). The binding parameters for scFv(EB3) were $K_{on} = 2.7 \times 10^5$ $Ms^{-1}$, $K_{off} = 2.7 \times 10^{-2}s^{-1}$ and $K_d = 99$ nM. SIP(EB3) exhibited a higher functional affinity and a reduced kinetic dissociation constant, as a result of avidity effects.

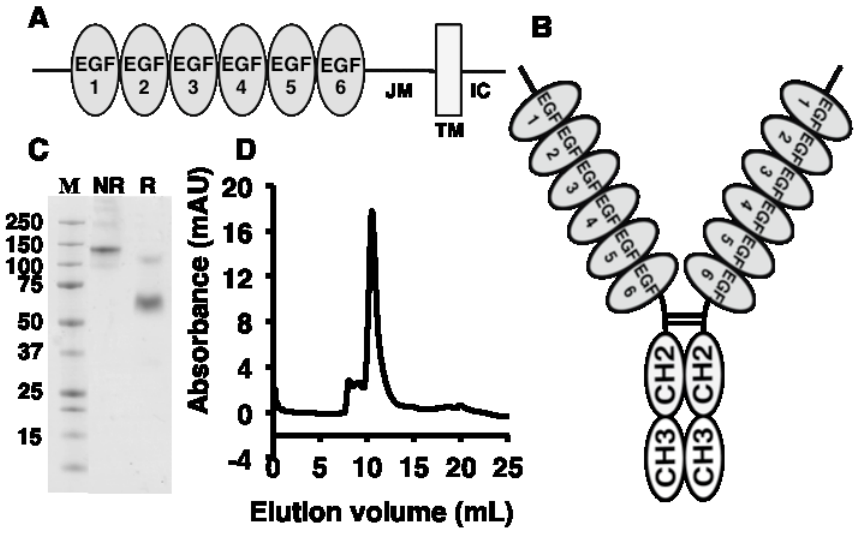


**Figure 1.** Recombinant fragment of human delta-like 1 homolog protein (DLK1) was expressed and characterized. (**A**) Schematic representation of DLK1 protein structure which comprises 6 epidermal growth factor (EGF)-like extracellular domains, a juxtamembrane region (JM), a transmembrane domain (TM) and a short intracellular region (IC). (**B**) Schematic representation of a DLK1-Fc fragment. Extracellular part of DLK comprising six EGF-like domain and a juxtamembrane region was fused to the CH2 and CH3 domains of the Fc part of IgG1. The fusion protein forms a covalent dimer. (**C**) SDS-PAGE profile of recombinant human DLK1-Fc fusion protein. M-marker; NR-DLK1-Fc under non-reducing conditions; R-DLK1-Fc under reducing conditions. (**D**) Size exclusion chromatography of the expressed DLK1-Fc fragment on Superdex S200 column.

**Table 1.** List of peptides obtained by tryptic digestion of the DLK1-Fc fusion protein.

| DLK1-Fc | Sequence | Start Sequence Position | End Sequence Position |
|---|---|---|---|
| 1 | AECFPACNPQNGFCEDDNVCR | 1 | 21 |
| 2 | KDGPCVINGSPCQHGGTCVDDEGR | 104 | 127 |
| 3 | DGPCVINGSPCQHGGTCVDDEGR | 105 | 127 |
| 4 | CRCPAGFIDK | 171 | 180 |
| 5 | CPAGFIDK | 173 | 180 |
| 6 | RALSPQQVTR | 225 | 234 |
| 7 | LPSGYGLAYR | 235 | 244 |
| 8 | KTPLLTEGQEPK | 272 | 283 |
| 9 | TPLLTEGQEPK | 273 | 283 |
| 10 | THTCPPCPAPELLGGPSVFLFPPKPK | 288 | 313 |
| 11 | DTLMISR | 314 | 320 |
| 12 | TPEVTCVVVDVSHEDPEVK | 321 | 339 |
| 13 | FNWYVDGVEVHNAK | 340 | 353 |
| 14 | EEQYNSTYR | 358 | 366 |
| 15 | VVSVLTVLHQDWLNGK | 367 | 382 |
| 16 | VVSVLTVLHQDWLNGKEYK | 367 | 385 |
| 17 | ALPAPIEK | 392 | 399 |

**Table 1.** *Cont.*

| DLK1-Fc | Sequence | Start Sequence Position | End Sequence Position |
|---|---|---|---|
| 18 | EPQVYTLPPSR | 410 | 420 |
| 19 | EPQVYTLPPSRDELTK | 410 | 425 |
| 20 | NQVSLTCLVK | 426 | 435 |
| 21 | GFYPSDIAVEWESNGQPENNYK | 436 | 457 |
| 22 | TTPPVLDSDGSFFLYSK | 458 | 474 |
| 23 | LTVDKSR | 475 | 481 |
| 24 | WQQGNVFSCSVMHEALHNHYTQK | 482 | 504 |
| 25 | SLSLSPGK | 505 | 512 |

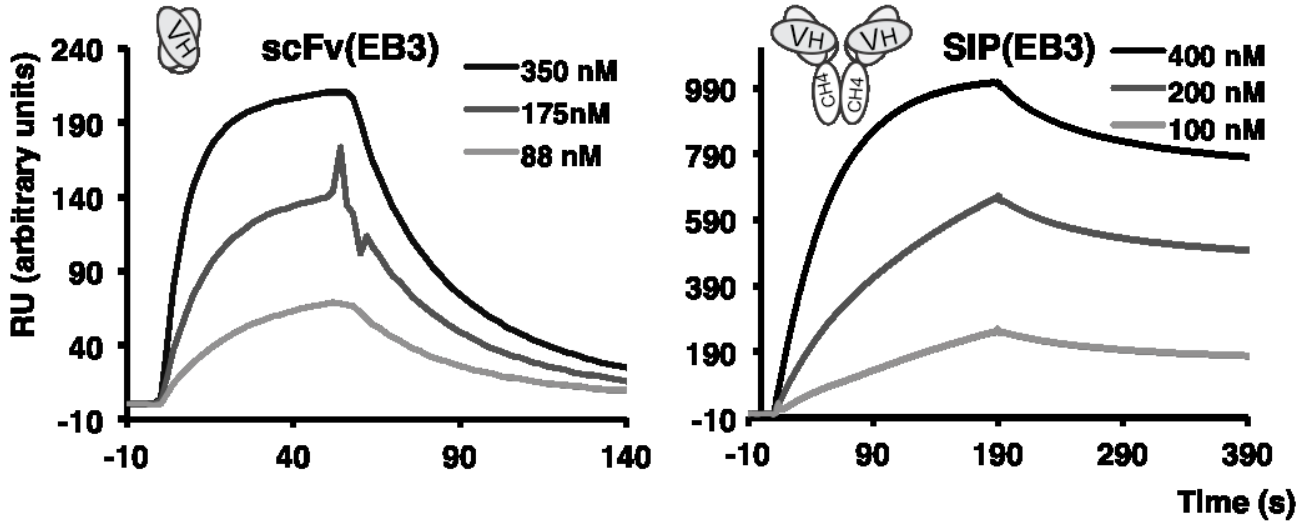


**Figure 2.** BIAcore profiles of the anti-DLK1 scFv antibody (left) and the SIP antibody (right) against human recombinant DLK1-Fc fusion protein.

*2.3. Immunofluorescence Findings*

A two-color immunofluorescence staining of a panel of freshly frozen sections from human healthy organs was performed using the SIP(EB3) antibody (green) and DAPI staining of nuclei (blue). The study revealed a weak expression of DLK1 in placenta, while the antigen was undetectable in the remaining 19/20 tested tissues, including adrenal gland and pancreas, which had previously been reported to express the antigen [14,15] (Figure 3).

Freshly frozen human tumors xenografted in nude mice were stained with the SIP(EB3) antibody (green) and with an anti-CD31 reagent, which recognizes vascular structures (red). Immunofluorescence microscopic analysis revealed that 8/9 tumors were strongly stained for DLK1 expression (786-0, SKRC-52, U87, SKOV-3, MDA-MB-231, H460, Caki1 and A-375), while Ramos lymphoma exhibited only a weak staining. SIP(F8), a clinical-stage antibody specific to the alternatively-spliced EDA domain of fibronectin, was used as a positive control. The F8 antibody exhibited a strong staining in 9/9 tumor xenografts, as expected based on previous reports of our group [39] (Figure 4). In addition, SIP(KSF), an antibody specific to hen-egg lysozyme and thus serving as negative control, did not exhibit any detectable staining in both healthy and tumor sections [46] (Figures 3 and 4).

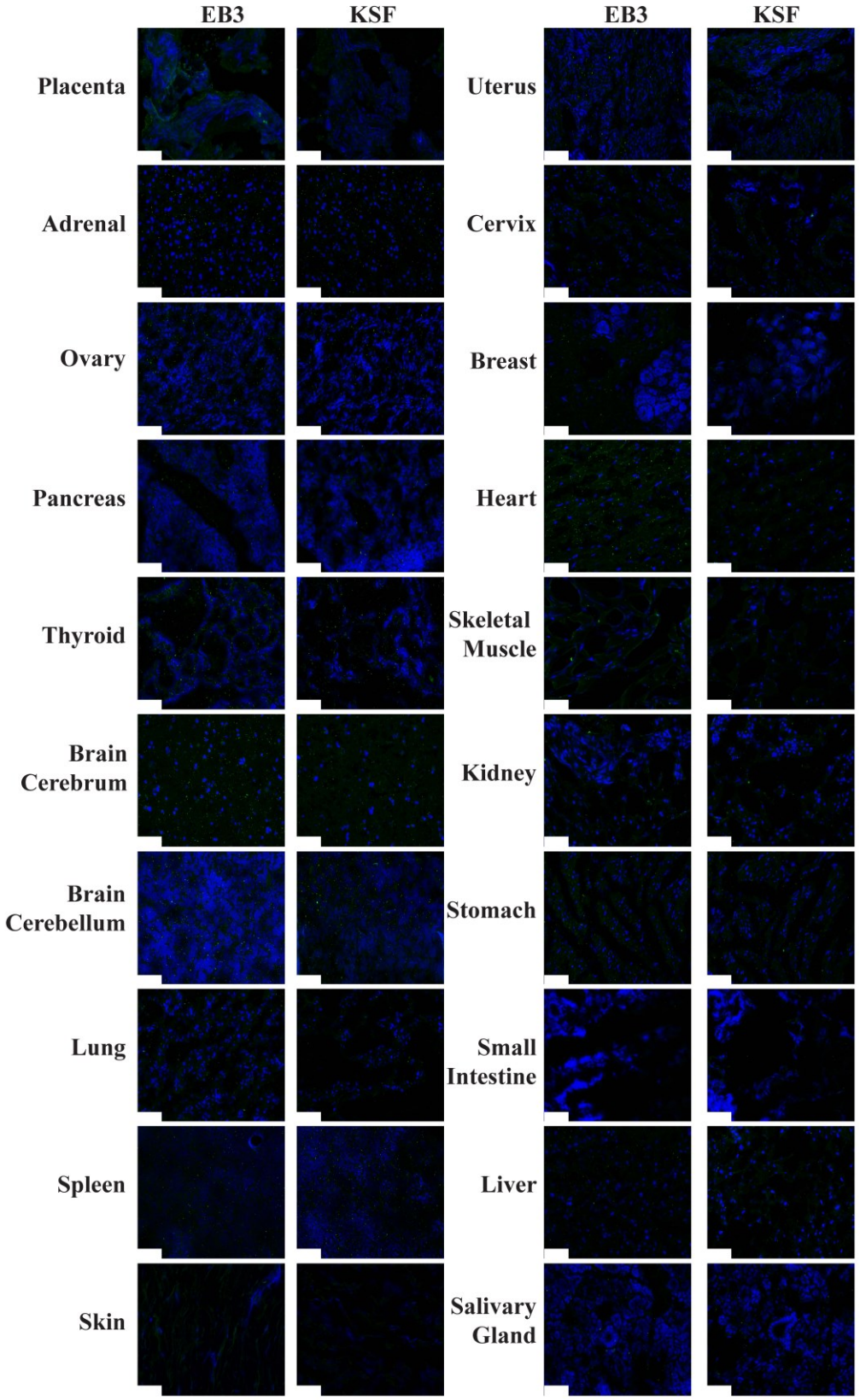


**Figure 3.** Immunofluorescence staining of human healthy tissues using small immune protein antibody formats SIP(KSF) and SIP(EB3). SIP antibodies are shown in green as they were detected using anti-human-IgE IgG antibody, which was further detected by Alexa Fluor 488 goat anti-rabbit IgG antibody. Cellular nuclei were stained with DAPI.

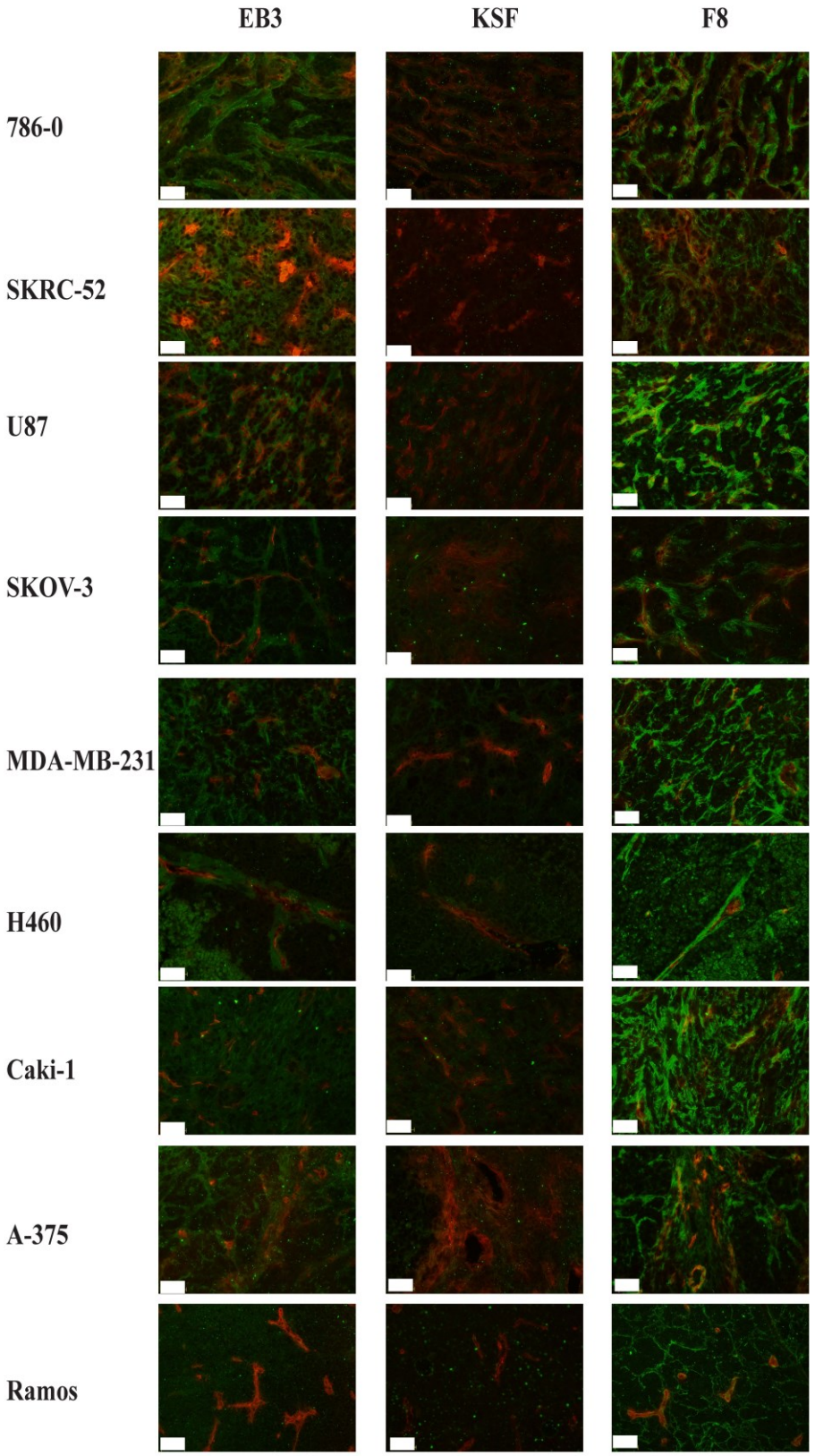


**Figure 4.** Immunofluorescence staining of human tumors xenografted in nude mice using SIP(KSF), SIP(EB3), SIP(F8) and anti-CD31 antibody. SIP antibodies are shown in green as they were detected using anti-human-IgE IgG antibody, which was then detected by Alexa Fluor 488 goat anti-rabbit IgG antibody. Endothelial cells of vessels are shown in red, as the anti-CD31 antibody was detected by donkey Alexa Fluor 594 anti-mouse IgG antibody.

*2.4.* In Vivo *Biodistribution Study*

The tumor targeting performance of the EB3 antibody in SIP format was evaluated in the U87 human glioblastoma model using a radioiodinated protein preparation (Figure 5). Surprisingly, the antibody did not exhibit a preferential accumulation at the tumor site, while the anti-EDA antibody, used as positive control, exhibited a tumor:blood ratio of 14 at the same time point. In spite of the strong immunochemical staining results observed with the EB3 antibody, it appears that other determinants (e.g., antigen abundance accessibility and stability, as well as antibody affinity [47]) may contribute to an efficient *in vivo* tumor targeting performance.

In our lab, we routinely measure immunoreactivity after labeling for those antibodies, for which reliable antigen resins can be produced, thanks to the availability of large amounts of antigen and of resin coupling protocols (e.g., extra-domains of fibronectin and of tenascin-C). Unfortunately, we could not produce antigen resin for DLK1 due to a low yield of antigen expression. Thus, we cannot exclude loss of immunoreactivity upon labeling.

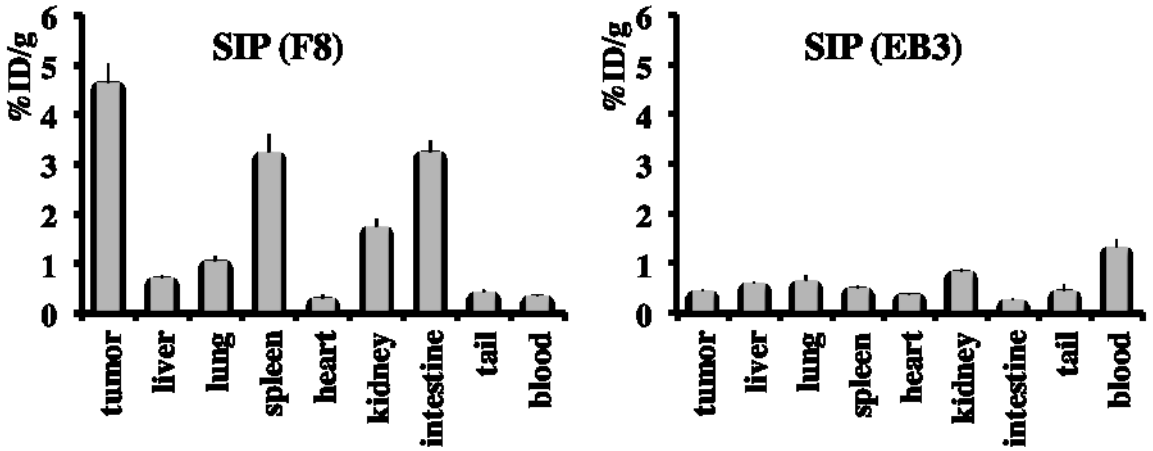


**Figure 5.** Radioiodinated preparations of SIP(F8) (left) and SIP(EB3) (right) were injected into nude mice, bearing subcutaneously-grafted U87 tumors. Twenty-four hours after intravenous administration, SIP(EB3) failed to localize to the neoplastic lesions *in vivo*. Results are expressed as percentage of injected dose per gram of tumor tissue (%ID/g).

Literature reports on the expression of DLK1 were based both on immunohistochemical analysis and on Northern blotting studies. These reports evidenced a strong expression of DLK1 in many fetal tissues [13], but absence in almost all healthy adult tissues, with the exception of Langerhans islets of pancreas and of the adrenal gland [14,15]. However, Kawakami and colleagues had previously documented DLK1 expression in proximal tubular cells of normal kidney tissue [36]. Protein Atlas analysis of DLK1 expression in various tissues revealed variable staining levels in pancreas and adrenal gland, depending of the antibody, which was used for the analysis. This variability can be explained by the fact that these antibodies recognize different epitopes. In fact, one antibody was specific for the extracellular part of DLK1 while two were specific for the intracellular domain. In particular, Protein Atlas evidences DLK1 mRNA expression in both placenta and adrenal gland. However, strong immunostaining of these tissues is only observed using antibodies raised against the intracellular part of the human DLK1. In fact, when an antibody specific to the extracellular domain of DLK1 is used, the staining is reported to be low in

both placenta and adrenal gland. This is in line with our findings of weak staining of placenta using SIP(EB3), which is specific to the extracellular domain of DLK1. In the case of adrenal gland, low abundance of the accessible DLK1 protein as well as the low affinity of SIP(EB3) may explain the absence of immunostaining using SIP(EB3). Also, two antibodies were polyclonal and different antigen staining patterns are sometimes observed when monoclonal antibodies area used [48]. In the literature, the expression of DLK1 is often limited to particular structures within an organ, as is the case in Langerhans islets of pancreas. It may therefore be possible that the lack of staining using SIP(EB3) stems from the absence of these specific structures in the tested tissues. Additionally, three gene-derived variants of DLK1 were observed as well as proteolytic fragments of the protein [30,49].

In our analysis, normal organs which were scored negative in immunofluorescence analysis included adrenal, ovary, pancreas, thyroid, brain cerebellum, brain cerebrum, lung, spleen, skin, uterus, cervix, breast, heart, skeletal muscle, kidney, stomach, small intestine, liver and salivary gland. The weak staining observed in placenta confirmed the ability of SIP(EB3) to recognize the cognate antigen human antigen in the freshly-frozen tissue microarray used for the study.

Tumor xenograft specimens stained with SIP(EB3) revealed abundant depositions of DLK1 in 786-0, SKRC-52, U87, SKOV-3, MDA-MB-231, H460, Caki-1 and A-375 cancers. In the majority of the cases (786-0, U87, SKOV-3. MDA-MB-231, H460 and A-375), a predominant stromal and vascular staining pattern was observed. The strongest staining intensity was observed for the 786-0 renal cell carcinoma tumor. Staining patterns of EB3 and F8 were similar for most tumors, but F8 generally gave a stronger signal in immunofluorescence, with the sole exception of 786-0 tumors. It is impossible to draw quantitative conclusions from these findings, as F8 is an affinity-matured antibody, with monomeric dissociation constant of 3 nM against its cognate antigen.

Protein Atlas analysis of DLK1 expression in human cancers revealed a positive staining only for a very small number of cases. The best results were observed in 4/12 lung cancer patients and only with one of the three antibodies that were used, with a nuclear staining pattern. The only human lung cancer xenograft (H460) studied in our analysis revealed a moderate staining around vascular structures (Figure 4). We found antigen expression in xenografted kidney cancer (786-0 and SKRC-52), while these malignancies were generally DLK1-negative in the Protein Atlas analysis. We have previously reported differences between our own findings and Protein Atlas reports for other components of the tumor stroma (e.g., TSP1, TSP2, MMP1, MMP2 and MMP3) [48,50]. These findings may be due to the fact that freshly-frozen specimens were always used in our studies. In general, the availability of new antibodies helps validate antigen expression patterns, an important feature when biomedical applications are planned.

Our findings of strong DLK1 expression in kidney cancer is in conflict with previous reports, which documented absence of DLK1 mRNA expression in renal cell carcinoma cell lines, including Caki-1 [36]. Similarly, we observed an intense antigen staining in U87 cell line, for which DLK mRNA was not detected in the Protein Atlas cell line analysis. The reasons for this discrepancy, at present, are not clear. In addition, DLK1 transcript was absent from the majority of human tumor cell lines derived from ovary, breast, skin and blood [32]. However, the corresponding tumors (SKOV-3, A-375 and MDA-MB-231) exhibited strong staining with EB3 antibody. These findings raise issues with respect to the sensitivity of previous mRNA detection methods or to the origin of the protein (e.g., fibroblast vs. tumor cell production). While mRNA expression analyses of the tested tissues may be indicative of protein's

presence, mRNA levels do not necessarily translate into protein [51,52]. Therefore, reagents highly specific to the protein, e.g., antibodies, are essential for characterizing protein expression in tissues.

In summary, we found that the newly-developed EB3 antibody strongly stains freshly frozen sections of most tumors, while exhibiting only a weak staining of placenta and no detectable staining of 19 other normal adult human tissues. As a result of this analysis, DLK1 appears to be one of the few tumor-associated antigens, which exhibit a striking contrast between a very restricted pattern of expression in normal organs and a pan-tumoral staining potential. However, the dissociation constant of EB3 (Kd = 99 nM) is not sufficient for pharmacodelivery applications (Figure 5). Also, DLK1 in the blood was reported in the literature, which may impair tumor targeting using SIP(EB3). This limitation, however, may be overcome with the dose elevation of the injected antibody. Better tumor targeting results could also be expected if the antibody was submitted to an affinity maturation procedure (in full analogy to what we had previously reported for the clinical-stage L19, F8 and F16 antibodies [39,53,54]) followed by testing in syngeneic tumor models.

## 3. Experimental Section

### *3.1. Cloning and Expression of Human DLK1-Fc Fusion Protein*

The human DLK1 gene was amplified from the human placenta cDNA library using 5'-GCT GAA TGC TTC CCG GCC TGC-3' forward and 5'- CTG GCC CTC GGT GAG GAG AGG-3' backward primers. The extracellular part of DLK1, comprising aminoacids 24-303 (Supplementary Figure S1), was amplified using 5'- TCC TCC TGT TCC TCG TCG CTG TGG CTA CAG GTG TGC ACT CGG CTG AAT GCT TCC CGG CCT GC-3' forward primer, and 5'- GTT TTG TCA CAA GAT TTG GGC TCC TGG CCC TCG GTG AGG AGA GG-3' backward primer. Hinge region, CH2 and CH3 domains of human IgG1 from the pcDNA3—L19—IgG1 vector [45] was amplified using 5'-GAG CCC AAA TCT TGT GAC AAA ACT CAC ACA TGC CCA CCG TGC CCA GCA CC-3' forward primer and 5'-TTT TCC TTT TGC GGC CGC TTA TTA CCC GGA GAC AGG GAG AGG C-3' backward primer. The PCR assembly of the two DNA fragments was performed using 5'-CCC AAG CTT GTC GAC CAT GGG CTG GAG CCT GAT CCT CCT GTT CCT CGT CGC TGT GGC-3' forward primer, and 5'-TTT TCC TTT TGC GGC CGC TTA TTA CCC GGA GAC AGG GAG AGG C-3' backward primer. This fragment was further inserted into a pCEP4 vector (Invitrogen) using HindIII-NotI restriction enzymes (NEB). The obtained vector was then used to transiently transfect human embryo kidney (HEK 293-EBNA) cells according to the established protocol [55]. Proteins were purified from the culture supernatant on Day 6 post-transfection, using protein A resin (Sino Biological), dialysed against PBS (pH = 7.4) and stored at −80 °C.

### *3.2. Mass Spectrometric Analysis of Human DLK1-Fc Fusion Protein*

Five micrograms of DLK1-Fc were diluted with MilliQ water, reduced with TCEP (Sigma) and alkylated with iodoacetamide (Thermo Fisher Scientific). The reaction was quenched with cysteine (Fluka), the samples diluted with trypsin digestion buffer (50 mM Tris-HCl, 1mM CaCl2, pH 8.0) and 0.08 µg sequencing grade-modified porcine trypsin (Promega) was added. Peptides were desalted,

purified and concentrated with C18 microcolumns (OMIXs tips, Agilent) according to the manufacturer's guidelines, lyophilized and stored at −20 °C.

Mass spectrometric analysis was carried out with the 4800 MALDI TOF/TOF Analyzer (AB Sciex, USA). The resulting spectra were processed and analyzed using the Global Protein Server Workstation version 3.6 (GPS Explorer, Applied Biosystems), which uses internal MASCOT version 2.1 (Matrix Sciences, London, UK). The MS/MS data were searched against a database of the DLK1-Fc expression constructs and all human proteins downloaded from the UniProt website. Peptides were considered correct calls when the confidence interval was greater than 95%.

### *3.3. Screening of Phage Display Libraries and Selection of the Antibody*

The recombinant DLK1-Fc fragment was biotinylated with EZ-link Sulfo-NHS-LC-biotin (Pierce) according to the manufacturer's instructions. Fourteen micrograms of the biotinylated DLK1-Fc fragment were captured by 60 mg of streptavidin-coated magnetic beads (Dynabeads, Invitrogen), followed by blocking with 2% bovine serum albumin (BSA) solution for 1 hour, at room temperature. After two washing steps, phage derived from the ETH2-GOLD library [44] were added to the DLK1-Fc-coated-beads and incubated for 3 h at room temperature under overhead rotation. Unbound phage particles were washed away with 5 washing steps with PBS-0.1% Tween followed by 2 washings with PBS. Elution of phage particles was performed using 100 mM solution of triethylamine. Subsequent TG1 *E.coli* infection and phage amplification was performed according to the established protocol [39]. Bacterial supernatants harboring soluble scFv fragments were screened by ELISA as published elsewhere [44]. In brief soluble scFv were detected using the anti-myc tag 9E10 mAb and anti-mouse horseradish peroxidase (HRP) immunoglobulins (Sigma-Aldrich) as secondary antibodies. Sixty microliters of BM-Blue POD substrate (Roche) were added to each well for detection by colorimetric reaction. The reaction was stopped by adding 30 µL of 1 M $H_2SO_4$. The absorbance was measured using a plate reader (VersaMax) by subtraction of value at wavelength 650 nm from 450 nm. Positive clones were further assessed for their ability to bind the immobilized antigen on a high-coating-density chip using surface plasmon resonance (SPR) on the BIAcore3000 instrument (GE Healthcare). The specificity of the isolated scFv to DLK1 over Fc domain was confirmed using ELISA and BIAcore analyses.

### *3.4. Characterization of scFv Antibody Fragments*

Single chain variable fragments were expressed in TG1 E.Coli and purified by affinity chromatography from the culture supernatant using Protein A Sepharose (Sino Biological) as described previously [44]. Purified scFvs were characterized by SDS-PAGE and size exclusion chromatography (SEC) on S75 Superdex column (GE Healthcare).

### *3.5. BIAcore Analysis*

Monomeric fraction of the scFv(EB3) from the SEC analysis was isolated and used for affinity measurement on the BIAcore CM5 chip coated with cognate antigen (DLK1-Fc), using BIAcore3000 instrument as described elsewhere [56]. Kinetic measurement of the scFv(EB3) was performed and binding curves were analyzed with the BIA Evaluation software.

### *3.6. Sequencing of scFv Genes*

The DNA was amplified by PCR using primers 5'-CAG GAA ACA GCT ATG ACC ATG ATT AC-3' and 5'-GAC GTT AGT AAA TGA ATT TTC TGT ATG AGG-3' (Sigma). Sequencing was performed by GATC Biotech (Germany) according to the standard Sanger method.

### *3.7. Cloning and Expression of Small Immune Proteins (SIP)*

Single chain variable fragments obtained from library screening were reformatted into a SIP format employing a previously described procedure [45,57]. In brief, the scFv sequence was fused in frame with the sequence of the CH4 domain of the human IgE secretory isoform IgE-S2 using overlap extension PCR. The DNA fragment was inserted into pcDNA3.1 vector using HindIII-NotI restriction enzymes. The obtained plasmid was used to transiently transfect Chinese hamster ovary cells (CHO) as described elsewhere [58]. On Day 6 post-transfection SIPs were purified from the culture supernatant by affinity chromatography using Protein A Sepharose.

### *3.8. Immunofluorescence on Frozen Tissue Sections*

Frozen human healthy tissue arrays were purchased from Amsbio (T6234700-5). Human tumor xenografts were grown subcutaneously and excised from BALB/c nude mice. Tumors were embedded in freezing medium (Microm) and stored at −80 °C until sectioned. Tissue sections (10 μm) were fixed for 10 min with ice-cold acetone, rehydrated with PBS and blocked with 20% FCS in PBS. Purified anti-DLK1 SIP(EB3) was applied to slices at a concentration of 5 μg/mL in 3% BSA. The CH4 domain of SIP(EB3) was detected with rabbit anti-human-IgE IgG (Dako), which was then detected by Alexa Fluor 488 goat anti-rabbit IgG antibody (Molecular Probes). Blood vessels in tumor xenografts were detected with mouse anti-CD31 antibody (Invitrogen) followed by donkey Alexa Fluor 594 anti-mouse IgG antibody (Molecular Probes). Nuclei were counterstained with DAPI (Invitrogen). All commercial binding reagents were diluted according to the manufacturer's recommendation in 3% BSA solution. Rinsing with PBS was performed between all incubation steps. Slides were mounted with Fluorescent mounting medium (Dako) and analyzed with a Zeiss AxioVision 4.7 image analysis software (Carl Zeiss AG).

### *3.9. Biodistribution Studies*

The i*n vivo* targeting performance of SIP fragments was evaluated by a quantitative biodistribution analysis as previously described [59]. Briefly, purified antibody preparations were radiolabeled with $^{125}$I using the Iodogen method [60,61] and injected into the tail vein of BALB/c nude mice bearing s.c. implanted U87 tumor (about 10 μg per mouse). Mice were sacrificed 24 h after injection. Organs were weighed and radioactivity was counted with a PackardCobra γ counter. Radioactivity content of representative organs was expressed as the percentage of the injected dose per gram of tissue (%ID/g).

## 4. Conclusions

Using combinatorial phage display libraries, we raised a fully human monoclonal antibody specific to DLK1. This antibody was used for an analysis of DLK1 expression in freshly frozen human healthy tissues as well as human tumor xenograft specimens. The analysis revealed that DLK1 may be considered as a target for antibody-mediated pharmacodelivery strategies, in view of its strong pan-tumoral staining, which is contrasted by a restricted expression pattern in healthy organs.

## Supplementary Materials

Supplementary materials can be accessed at: http://www.mdpi.com/2073-4468/4/2/71/s1.

## Acknowledgments

Financial support from ETH Zürich, the Swiss National Science Foundation, the Kommission für Technologie und Innovation (KTI MedTech Award) and the European Union (PRIAT FP7 Project) is gratefully acknowledged. Authors would like to thank Francesca Pretto for her help with the biodistribution study.

## Author Contributions

EB and DN wrote the manuscript and designed the study. EB performed the experimental work. DR performed the MS analysis.

## Conflicts of Interest

Authors declare no conflict of interest.

## References

1. Aggarwal, S. What's fueling the biotech engine—2011 to 2012. *Nat. Biotech.* **2012**, *30*, 1191–1197.
2. Walsh, G. Biopharmaceutical benchmarks 2014. *Nat. Biotech.* **2014**, *32*, 992–1000.
3. Shim, H. One target, different effects: A comparison of distinct therapeutic antibodies against the same targets. *Exp. Mol. Med.* **2011**, *43*, 539–549.
4. Wang, Y.; Sul, H.S. Ectodomain Shedding of Preadipocyte Factor 1 (Pref-1) by Tumor Necrosis Factor Alpha Converting Enzyme (TACE) and Inhibition of Adipocyte Differentiation. *Mol. Cell. Biol.* **2006**, *26*, 5421–5435.
5. Laborda, J.; Sausville, E.A.; Hoffman, T.; Notario, V. dlk, a putative mammalian homeotic gene differentially expressed in small cell lung carcinoma and neuroendocrine tumor cell line. *J. Biol. Chem.* **1993**, *268*, 3817–3820.
6. Baladrón, V.; Ruiz-Hidalgo, M.J.; Nueda, M.L.; Díaz-Guerra, M.J.M.; García-Ramírez, J.J.; Bonvini, E.; Gubina, E.; Labord, J. dlk acts as a negative regulator of Notch1 activation through interactions with specific EGF-like repeats. *Exp. Cell Res.* **2005**, *303*, 343–359.

7. Nueda, M.-L.; Baladrón, V.; Sánchez-Solana, B.; Ballesteros, M.-Á.; Laborda, J. The EGF-like Protein dlk1 Inhibits Notch Signaling and Potentiates Adipogenesis of Mesenchymal Cells. *J. Mol. Biol.* **2007**, *367*, 1281–1293.
8. Li, L.; Forman, S.J.; Bhatia, R. Expression of DLK1 in hematopoietic cells results in inhibition of differentiation and proliferation. *Oncogene* **2005**, *24*, 4472–4476.
9. Smas, C.M.; Sul, H.S. Pref-1, a protein containing EGF-like repeats, inhibits adipocyte differentiation. *Cell* **1993**, *73*, 725–734.
10. Andersen, D.C.; Petersson, S.J.; Jørgensen, L.H.; Bollen, P.; Jensen, P.B.; Teisner, B.; Schroeder, H.D.; Jensen, C.H. Characterization of DLK1+ Cells Emerging During Skeletal Muscle Remodeling in Response to Myositis, Myopathies, and Acute Injury. *Stem Cells* 2009, *27*, 898–908.
11. Tanimizu, N.; Nishikawa, M.; Saito, H.; Tsujimura, T.; Miyajima, A. Isolation of hepatoblasts based on the expression of dlk/pref-1. *Journal of Cell Science* **2003**, *116*, 1775-1786.
12. Yevtodiyenko, A.; Schmidt, J.V. Dlk1 expression marks developing endothelium and sites of branching morphogenesis in the mouse embryo and placenta. *Dev. Dynam.* **2006**, *235*, 1115–1123.
13. Floridon, C.; Jensen, C.H.; Thorsen, P.; Nielsen, O.; Sunde, L.; Westergaard, J.G.; Thomsen, S.G.; Teisner, B. Does Fetal antigen 1 (FA1) identify cells with regenerative, endocrine and neuroendocrine potentials? A study of FA1 in embryonic, fetal, and placental tissue and in maternal circulation. *Differentiation* **2000**, *66*, 49–59.
14. Jensen, C.H.; Krogh, T.N.; Højrup, P.; Clausen, P.P.; Skjødt, K.; Larsson, L.-I.; Enghild, J.J.; Teisner, B. Protein Structure of Fetal Antigen 1 (FA1). *Eur. J. Biochem.* **1994**, *225*, 83–92.
15. Jensen, C.H.; Teisner, B.; Højrup, P.; Rasmussen, H.B.; Madsen, O.D.; Nielsen, B.; Skjødt, K. Studies on the isolation, structural analysis and tissue localization of fetal antigen 1 and its relation to a human adrenal-specific cDNA, pG2. *Hum. Reprod.* **1993**, *8*, 635–641.
16. Van Limpt, V.; Chan, A.; Caron, H.; Van Sluis, P.; Boon, K.; Hermus, M.-C.; Versteeg, R. SAGE analysis of neuroblastoma reveals a high expression of the human homologue of the Drosophila Delta gene. *Med. Pediatr. Oncol.* **2000**, *35*, 554–558.
17. Harel, A.; Dalah, I.; Pietrokovski, S.; Safran, M.; Lancet, D. Omics data management and annotation. In *Bioinformatics for Omics Data*; Mayer, B., Ed.; Humana Press: New York, NY, USA, 2011; Volume 719, pp. 71–96.
18. Traustadottir, G.A.; Kosmina, R.; Sheikh, S.P.; Jensenab, C.H.; Andersen, D.C. Preadipocytes proliferate and differentiate under the guidance of Delta-like 1 homolog (DLK1). *Adipocyte* **2013**, *2*, 272–275.
19. Surmacz, B.; Noisa, P.; Risner-Janiczek, J.R.; Hui, K.; Ungless, M.; Cui, W.; Li, M. DLK1 promotes neurogenesis of human and mouse pluripotent stem cell-derived neural progenitors via modulating Notch and BMP signalling. *Stem Cell Rev.* **2012**, *8*, 459–471.
20. Moon, Y.S.; Smas, C.M.; Lee, K.; Villena, J.A.; Kim, K.-H.; Yun, E.J.; Sul, H.S. Mice Lacking Paternally Expressed Pref-1/Dlk1 Display Growth Retardation and Accelerated Adiposity. *Mol. Cell. Biol.* **2002**, *22*, 5585–5592.
21. Waddell, J.N.; Zhang, P.; Wen, Y.; Gupta, S.K.; Yevtodiyenko, A.; Schmidt, J.V.; Bidwell, C.A.; Kumar, A.; Kuang, S. Dlk1 Is Necessary for Proper Skeletal Muscle Development and Regeneration. *PLoS One* **2010**, *5*, e15055.

22. Raghunandan, R.; Ruiz-Hidalgo, M.; Jia, Y.; Ettinger, R.; Rudikoff, E.; Riggins, P.; Farnsworth, R.; Tesfaye, A.; Laborda, J.; Bauer, S.R. Dlk1 influences differentiation and function of B lymphocytes. *Stem Cells Dev.* **2008**, *17*, 495–507.
23. Huang, J.; Zhang, X.; Zhang, M.; Zhu, J.-D.; Zhang, Y.-L.; Lin, Y.; Wang, K.-S.; Qi, X.-F.; Zhang, Q.; Liu, G.-Z.; *et al.* Up-regulation of DLK1 as an imprinted gene could contribute to human hepatocellular carcinoma. *Carcinogenesis* **2007**, *28*, 1094–1103.
24. Jin, Z.-H.; Yang, R.-J.; Dong, B.; Xing, B. Progenitor gene DLK1 might be an independent prognostic factor of liver cancer. *Exp. Opin. Biol. Ther.* **2008**, *8*, 371–377.
25. Chi Sabins, N.; Taylor, J.L.; Fabian, K.P.L.; Appleman, L.J.; Maranchie, J.K.; Stolz, D.B.; Storkus, W.J. DLK1: A Novel Target for Immunotherapeutic Remodeling of the Tumor Blood Vasculature. *Mol. Ther.* **2013**, *21*, 1958–1968.
26. Van Limpt, V.E.; Chan, A.J.; Van Sluis, P.G.; Caron, H.N.; van Noesel, C.J.M.; Versteeg, R. High delta-like 1 expression in a subset of neuroblastoma cell lines corresponds to a differentiated chromaffin cell type. *Int. J. Cancer* **2003**, *105*, 61–69.
27. López-Terrada, D.; Gunaratne, P.H.; Adesina, A.M.; Pulliam, J.; Hoang, D.M.; Nguyen, Y.; Mistretta, T.-A.; Margolin, J.; Finegold, M.J. Histologic subtypes of hepatoblastoma are characterized by differential canonical Wnt and Notch pathway activation in DLK+ precursors. *Hum. Pathol.* **2009**, *40*, 783–794.
28. Qi, X.; Chen, Z.; Liu, D.; Cen, J.; Gu, M. Expression of Dlk1 gene in myelodysplastic syndrome determined by microarray, and its effects on leukemia cells. *Int. J. Mol. Med.* **2008**, *22*, 61–68.
29. Sakajiri, S.; O'kelly, J.; Yin, D.; Miller, C.W.; Hofmann, W.K.; Oshimi, K.; Shih, L.-Y.; Kim, K.-H.; Sul, H.S.; Jensen, C.H.; *et al.* Dlk1 in normal and abnormal hematopoiesis. *Leukemia* **2005**, *19*, 1404–1410.
30. Altenberger, T.; Bilban, M.; Auer, M.; Knospc, E.; Wolfsbergerc, S.; Gartnera, W.; Minevaa, I.; Zielinskid, C.; Wagnera, L.; Lugera, A. Identification of DLK1 variants in pituitary- and neuroendocrine tumors. *Biochem. Biophys. Res. Commun*. **2006**, *340*, 995–1005.
31. Yanai, H.; Nakamura, K.; Hijioka, S.; Kamei, A.; Ikari, T.; Ishikawa, Y.; Shinozaki, E.; Mizunuma, N.; Hatake, K.; Miyajima, A. Dlk-1, a cell surface antigen on foetal hepatic stem/progenitor cells, is expressed in hepatocellular, colon, pancreas and breast carcinomas at a high frequency. *J. Biochem.* **2010**, *148*, 85–92.
32. Park, Y.W.; Jo, K.; Lee, D.; Yu, J.; Park, J.H.; Park, C.-W.; Kim, E.J.; Park, Y.J. Method for inhibiting cancer metastasis by administration of the extracellular domain DLK1 or a DLK1-FC fusion protein. US 8785392 B2, 22 July 2014.
33. Yu, F.; Hao, X.; Zhao, H.; Ge, C.; Yao, M.; Yang, S.; Li, J. Delta-like 1 contributes to cell growth by increasing the interferon-inducible protein 16 expression in hepatocellular carcinoma. *Liver Int.* **2010**, *30*, 703–714.
34. Kim, Y.; Lin, Q.; Zelterman, D.; Yun, Z. Hypoxia-regulated delta-like 1 homologue enhances cancer cell stemness and tumorigenicity. *Cancer Res.* **2009**, *69*, 9271–9280.
35. Orr, B.; Grace, O.C.; Brown, P.; Riddick, A.C.P.; Stewart, G.D.; Franco, O.E.; Hayward, S.W.; Thomson, A.A. Reduction of pro-tumorigenic activity of human prostate cancer-associated fibroblasts using Dlk1 or SCUBE1. *Dis. Model. Mech*. **2013**, *6*, 530–536.

36. Kawakami, T.; Chano, T.; Minami, K.; Okabe, H.; Okada, Y.; Okamoto, K. Imprinted DLK1 is a putative tumor suppressor gene and inactivated by epimutation at the region upstream of GTL2 in human renal cell carcinoma. *Hum. Mol. Genet.* **2006**, *15*, 821–830.
37. Nueda, M.L.; Naranjo, A.I.; Baladron, V.; Labordab, J. The proteins DLK1 and DLK2 modulate NOTCH1-dependent proliferation and oncogenic potential of human SK-MEL-2 melanoma cells. *Biochim. Biophys. Acta* **2014**, *1843*, 2674–2684.
38. Uhlen, M.; Oksvold, P.; Fagerberg, L.; Lundberg, E.; Jonasson, K.; Forsberg, M.; Zwahlen, M.; Kampf, C.; Wester, K.; Hober, S. *et al.* Towards a knowledge-based Human Protein Atlas. *Nat Biotech.* **2010**, *28*, 1248–1250.
39. Villa, A.; Trachsel, E.; Kaspar, M.; Schliemann, C.; Sommavilla, R.; Rybak, J.-N.; Rösli, C.; Borsi, L.; Neri, D. A high-affinity human monoclonal antibody specific to the alternatively spliced EDA domain of fibronectin efficiently targets tumor neo-vasculature *in vivo*. *Int. J. Cancer* **2008**, *122*, 2405–2413.
40. Schwager, K.; Villa, A.; Rosli, C.; Neri, D.; Rösli-Khabas, M.; Moser, G. A comparative immunofluorescence analysis of three clinical-stage antibodies in head and neck cancer. *Head Neck Oncol.* **2011**, *3*, 25.
41. Schliemann, C.; Neri, D. Antibody-based targeting of the tumor vasculature. *Biochim. Biophys. Acta* **2007**, *1776*, 175–192.
42. Weber, M.; Bujak, E.; Putelli, A.; Villa, A.; Matasci, M.; Gualandi, L.; Hemmerle, T.; Wulhfard, S.; Neri, D. A highly functional synthetic phage display library containing over 40 billion human antibody clones. *PLoS One* **2014**, *9*, e100000.
43. Huston, J.S.; Levinson, D.; Mudgett-Hunter, M.; Tai, M.S.; Novotný, J.; Margolies, M.N.; Ridge, R.J.; Bruccoleri, R.E.; Haber, E.; Crea, R. Protein engineering of antibody binding sites: recovery of specific activity in an anti-digoxin single-chain Fv analogue produced in *Escherichia coli*. *Proc. Natl. Acad. Sci. USA* **1988**, *85*, 5879–5883.
44. Silacci, M.; Brack, S.; Schirru, G.; Mårlind, J.; Ettorre, A.; Merlo, A.; Viti, F.; Neri, D. Design, construction, and characterization of a large synthetic human antibody phage display library. *Proteomics* **2005**, *5*, 2340–2350.
45. Borsi, L.; Balza, E.; Bestagno, M.; Castellani, P.; Carnemolla, B.; Biro, A.; Leprini, A.; Sepulveda, J.; Burrone, O.; Neri, D.; *et al.* Selective targeting of tumoral vasculature: comparison of different formats of an antibody (L19) to the ED-B domain of fibronectin. *Int. J. Cancer* **2002**, *102*, 75–85.
46. Frey, K.; Zivanovic, A.; Schwager, K.; Neri, D. Antibody-based targeting of interferon-alpha to the tumor neovasculature: A critical evaluation. *Integr. Biol.* **2011**, *3*, 468–478.
47. Schliemann, C.; Neri, D. Antibody-based vascular tumor targeting. *Recent Results Cancer Res.* **2010**, *180*, 201–216.
48. Pfaffen, S.; Hemmerle, T.; Weber, M.; Neri, D. Isolation and characterization of human monoclonal antibodies specific to MMP-1A, MMP-2 and MMP-3. *Exp. Cell Res.* **2010**, *316*, 836–847.
49. Deiuliis, J.A.; Li, B.; Lyvers-Peffer, P.A.; Moellera, S.J.; Lee, K. Alternative splicing of delta-like 1 homolog (DLK1) in the pig and human. *Comp. Biochem. Physi. B* **2006**, *145*, 50–59.
50. Bujak, E.; Pretto, F.; Ritz, D.; Gualandi, L.; Wulhfard, S.; Neri, D. Monoclonal antibodies to murine thrombospondin-1 and thrombospondin-2 reveal differential expression patterns in cancer and low antigen expression in normal tissues. *Exp. Cell Res.* **2014**, *327*, 135–145.

51. Anderson, L.; Seilhamer, J. A comparison of selected mRNA and protein abundances in human liver. *Electrophoresis* **1997**, *18*, 533–537.
52. Gygi, S.P.; Rochon, Y.; Franza, B.R.; Aebersold, R. Correlation between protein and mRNA abundance in yeast. *Mol. Cell. Biol.* **1999**, *19*, 1720–1730.
53. Pini, A.; Viti, F.; Santucci, A.; Carnemoll, B.; Zardi, L.; Neri, P.; Neri, D. Design and Use of a Phage Display Library: Human antibodies with subnanomolar affinity against a marker of angiogenesis eluted from a two-dimensional gel. *J. Biol. Chem.* **1998**, *273*, 21769–21776.
54. Brack, S.S.; Silacci, M.; Birchler, M.; Neri, D. Tumor-Targeting Properties of Novel Antibodies Specific to the Large Isoform of Tenascin-C. *Clin. Cancer Res.* **2006**, *12*, 3200–3208.
55. Bujak, E.; Matasci, M.; Neri, D.; Wulhfard, S. Reformatting of scfv antibodies into the scfv-fc format and their downstream purification. In *Monoclonal Antibodies*; Ossipow, V., Fischer, N., Eds.; Humana Press: New York, NY, USA, 2014; Volume 1131, pp. 315–334.
56. Silacci, M.; Brack, S.; Spath, N.; Buck, A.; Hillinger, S.; Arni, S.; Weder, W.; Zardi, L.; Neri, D. Human monoclonal antibodies to domain C of tenascin-C selectively target solid tumors *in vivo*. *Protein Eng. Des. Sel.* **2006**, *19*, 471–478.
57. Zuberbühler, K.; Palumbo, A.; Bacci, C.; Giovannoni, L.; Sommavilla, R.; Kaspar, M.; Trachsel, E.; Neri, D. A general method for the selection of high-level scFv and IgG antibody expression by stably transfected mammalian cells. *Protein Eng. Des. Sel.* **2009**, *22*, 169–174.
58. List, T.; Neri, D. Biodistribution studies with tumor-targeting bispecific antibodies reveal selective accumulation at the tumor site. *mAbs* **2012**, *4*, 775–783.
59. Tarli, L.; Balza, E.; Viti, F.; Borsi, L.; Castellani, P.; Berndorff, D.; Dinkelborg, L.; Neri, D.; Zardi, L. A High-Affinity Human Antibody That Targets Tumoral Blood Vessels. *Blood* **1999**, *94*, 192–198.
60. Fraker, P.J. Reprint of "Protein and Cell Membrane Iodinations with a Sparingly Soluble Chloroamide, 1,3,4,6-Tetrachloro-3a,6a-Diphenylglycoluril". *Biochem. Biophys. Res. Commun.* **2012**, *425*, 510–518.
61. Salacinski, P.R.P.; Mclean, C.; Sykes, J.E.C.; Clement-Jones, V.V.; Lowry, P.J. Iodination of proteins, glycoproteins, and peptides using a solid-phase oxidizing agent, 1,3,4,6-tetrachloro-3α,6α-diphenyl glycoluril (Iodogen). *Anal. Biochem.* **1981**, *117*, 136–146.